

Electron-Transfer Properties of Active Aldehydes of Thiamin Coenzyme Models, and Mechanism of Formation of the Reactive Intermediates

Ikuro Nakanishi, Shinobu Itoh, and Shunichi Fukuzumi*^[a]

Abstract: The active aldehydes $2\mathbf{a}-\mathbf{c}^-$ derived from the reaction of 3-benzylthiazolium salts ($1\mathbf{a}^+$: 3-benzyl-4-methylthiazolium bromide, $1\mathbf{b}^+$: 3-benzyl-4,5-dimethylthiazolium bromide, $1\mathbf{c}^+$: 3-benzylthiazolium bromide) with *o*-tolualdehyde in the presence of DBU (1,8-diazabicyclo[5.4.0]undec-7-ene) are stable in deaerated MeCN at 298 K because of the steric bulkiness of the *o*-methyl group, which prohibits benzoin condensation with a second aldehyde molecule. The one-electron oxidation of fourteen different active aldehydes ($2\mathbf{a}-\mathbf{n}^-$) derived from various aldehydes occurs at -0.98 to -0.77 V vs. SCE in deaerated MeCN at 298 or 233 K

and leads to formation of the corresponding radical intermediates ($2\mathbf{a}-\mathbf{n}^\bullet$), which have been characterized by electron spin resonance (ESR) spectroscopy. The rapid rates of electron exchange between $2\mathbf{a}-\mathbf{c}^-$ and $2\mathbf{a}-\mathbf{c}^\bullet$ were determined by the linewidth variations of the ESR spectra of $2\mathbf{a}-\mathbf{c}^\bullet$ in the presence of different concentrations of $2\mathbf{a}-\mathbf{c}^-$, demonstrating the efficient electron-transfer properties of the active aldehydes. The electron transfer from $2\mathbf{a}^-$ to an

Keywords: coenzymes • cyclic voltammetry • ESR spectroscopy • radicals • thiamin

outer-sphere one-electron oxidant, $[\text{Co}^{\text{II}}(\text{phen})_3]^{2+}$ (phen = 1,10-phenanthroline), whose one-electron reduction potential ($E_{\text{red}}^\circ = -0.97$ V) is about the same as the one-electron oxidation potential of $2\mathbf{a}^-$ ($E_{\text{ox}}^\circ = -0.96$ V), occurs efficiently to yield the corresponding Co^{I} complex. The observed rate constants for formation of $[\text{Co}^{\text{I}}(\text{phen})_3]^+$ agree with those for formation of the active aldehyde examined independently. This agreement indicates that rate-determining formation of $2\mathbf{a}^-$, which is a very strong reductant, precedes the highly efficient electron transfer from $2\mathbf{a}^-$ to $[\text{Co}^{\text{II}}(\text{phen})_3]^{2+}$.

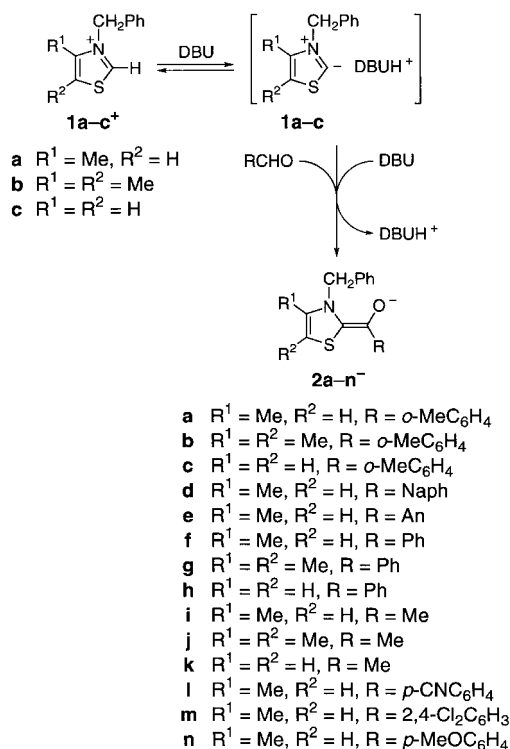
Introduction

Thiamin diphosphate (ThDP) is the coenzyme for a number of important biochemical reactions, catalysing the decarboxylation of α -keto acids and the transfer of acyl groups.^[1–3] The conjugate base of 2-(α -hydroxyethyl)ThDP, which is an acyl carbanion equivalent, called an active aldehyde, is known to play an essential role in the catalysis of ThDP-dependent enzymes. The active aldehyde has ability to mediate an efficient electron transfer to various physiological electron acceptors, such as, for example, lipoamide in pyruvate dehydrogenase multienzyme complex,^[4] flavin adenine dinucleotide (FAD) in pyruvate oxidase,^[5] and the Fe_4S_4 cluster in pyruvate-ferredoxin oxidoreductase.^[6] In this context, chemical models of thiamin coenzyme have been studied extensively by means of simple thiazolium ions, providing valuable information about the elementary steps of ThDP-dependent

enzymatic reactions.^[7–17] However, the generated active aldehyde readily undergoes acyloin-type condensation with a second pyruvate or aldehyde molecule in the absence of the oxidizing agents.^[18, 19] This instability of the active aldehydes has so far precluded the direct detection of the intermediates or determination of fundamental redox properties of the active aldehydes such as the one-electron redox potentials and the intrinsic barrier for the electron-transfer reactions.^[20]

We report herein the direct detection of radical intermediates ($2\mathbf{a}-\mathbf{l}^\bullet$) of active aldehydes ($2\mathbf{a}-\mathbf{l}^-$) derived from three different 3-benzylthiazolium salts ($1\mathbf{a}-\mathbf{c}^+$) and eight different aldehydes in the presence of 1,8-diazabicyclo[5.4.0]undec-7-ene (DBU) in acetonitrile (MeCN) by using electron spin resonance (ESR), and the first and second one-electron oxidation potentials of fourteen different active aldehydes ($2\mathbf{a}-\mathbf{n}^-$; Scheme 1).^[21] This has been made possible by using active aldehydes stabilized by steric bulk, or by lowering the reaction temperature. The rapid electron exchange rates between $2\mathbf{a}-\mathbf{c}^-$ and $2\mathbf{a}-\mathbf{c}^\bullet$ can be determined by the linewidth variations of the ESR spectra depending on different concentrations of the active aldehydes. This study also reports the kinetic investigation of an efficient electron transfer from an active aldehyde to an outer-sphere one-electron oxidant, $[\text{Co}^{\text{II}}(\text{phen})_3]^{2+}$ (phen = 1,10-phenanthroline), as well as the

[a] Prof. Dr. S. Fukuzumi, I. Nakanishi, Assoc. Prof. Dr. S. Itoh
Department of Material and Life Science
Graduate School of Engineering, Osaka University
Suita, Osaka 565-0871 (Japan)
Fax: (+81) 6-6879-7370
E-mail: fukuzumi@chem.eng.osaka-u.ac.jp



Scheme 1. Formation of active aldehyde from 3-benzylthiazolium salts **1a-c⁺** and aldehydes (RCHO) in the presence of DBU.

formation of active aldehydes. The highly negative oxidation potentials of active aldehydes and the spin distribution of the intermediate radicals determined for the first time in this study provide comprehensive and corroborative understanding of the ThDP-dependent electron-transport systems as well as valuable mechanistic insight into the enzymatic reactions.

Results and Discussion

One-electron oxidation potentials of active aldehydes: The active aldehydes **2a-c⁻** derived from the series of 3-ben-

Abstract in Japanese:

塩基存在下、チアミン補酵素モデル化合物である3-ベンジルチアゾリウム塩と種々のアルデヒドから生成する活性アルデヒド中間体を安定化することに成功し、その酸化電位を決定した。得られた酸化電位は非常に低く、活性アルデヒド中間体が極めて強力な還元剤として作用することがわかった。また、活性アルデヒドを一電子酸化することにより生成するラジカル中間体の電子スピン共鳴(ESR)法による検出に初めて成功し、その電子構造を明らかにした。さらに、このラジカル中間体のESRスペクトルの活性アルデヒド濃度による線幅変化から、活性アルデヒドとラジカル中間体との電子交換速度定数および電子移動の再配列エネルギーを決定し、活性アルデヒドが極めて効率のよい電子供与体として作用することを明らかにした。実際、活性アルデヒドからトリス(1,10-フェナントロリン)コバルト(II)錯体への電子移動反応速度定数は、活性アルデヒド生成の速度定数とよく一致し、いったん活性アルデヒドが生成すると、コバルト(II)錯体への電子移動は非常に速く、活性アルデヒドの生成が律速段階となって、電子受容体の電子移動が極めて効率よく進行することがわかった。

zylthiazolium salts (**1a-c⁺**) with *o*-tolualdehyde (*o*-MeC₆H₄CHO) in the presence of DBU are stable enough for it to be possible to determine redox potentials by cyclic voltammetry (CV) measurements in MeCN at 298 K. This is because the steric bulk of the *o*-methyl group prevents the benzoin condensation with a second aldehyde molecule. Thus, a cyclic voltammogram recorded for **2a⁻** prepared in situ by addition of neat DBU (1.0 × 10⁻² M) to a MeCN solution containing **1a⁺** (5.0 × 10⁻³ M), *o*-MeC₆H₄CHO (0.25 M), and tetra-*n*-butylammonium perchlorate (TBAP) (0.10 M) as a supporting electrolyte at 298 K exhibits two reversible one-electron redox peaks at $E_{\text{ox}(1)}^{\circ} = -0.96$ and $E_{\text{ox}(2)}^{\circ} = -0.52$ V vs. SCE (Figure 1).^[22] The reversible CV waves can be observed only

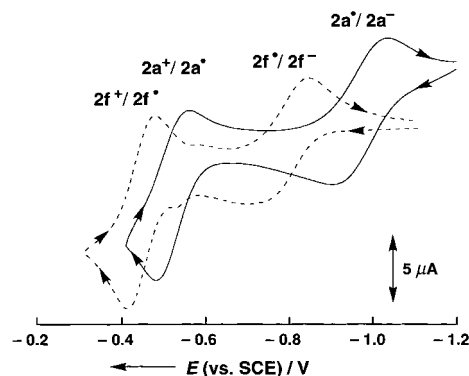


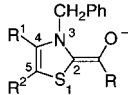
Figure 1. Cyclic voltammograms of **2a⁻**, derived from **1a⁺** (5.0 × 10⁻³ M), *o*-tolualdehyde (0.25 M), and DBU (1.0 × 10⁻² M), at 298 K (solid curve), and of **2f⁻**, derived from **1a⁺** (5.0 × 10⁻³ M), benzaldehyde (0.25 M), and DBU (1.0 × 10⁻² M), at 233 K (dashed curve) in deaerated MeCN containing 0.10 M TBAP. Sweep rate 0.10 V s⁻¹.

in the presence of all the components together, that is, **1a⁺**, *o*-MeC₆H₄CHO, and DBU. This indicates that it is not the parent compound but the active aldehyde **2a⁻** that undergoes the electrochemical redox reactions. The reversible one-electron redox waves were also observed at 298 K for active aldehydes **2d⁻** and **2e⁻**, derived from **1a⁺** with 1-naphthaldehyde (R = Naph) and 9-anthraldehyde (R = An), respectively; the $E_{\text{ox}(1)}^{\circ}$ and $E_{\text{ox}(2)}^{\circ}$ values are listed in Table 1. However, no CV peaks can be observed for active aldehydes derived from other aldehydes, which are unstable at 298 K.

The benzoin condensation which causes disappearance of the active aldehyde may be retarded by lowering the temperature to 233 K. In fact, the reversible CV waves for active aldehydes derived from other aldehydes can be observed at 233 K. A typical example of the CV wave of **2f⁻** at 233 K derived from **1a⁺** and benzaldehyde (PhCHO) in the presence of DBU is shown in Figure 1. The first oxidation potentials $E_{\text{ox}(1)}^{\circ}$ and the second oxidation potentials $E_{\text{ox}(2)}^{\circ}$ of various active aldehydes (**2a-n⁻**) thus obtained are summarized in Table 1.

As shown in Table 1, the parent aldehydes have little effect on the $E_{\text{ox}(1)}^{\circ}$ values. The $E_{\text{ox}(1)}^{\circ}$ values of the active aldehydes are nearly the same (-0.93 to -0.98 V) irrespective of the parent aldehyde, except for those from PhCHO (**2f-h⁻**) and *p*-cyanobenzaldehyde (*p*-CNC₆H₄CHO) (**2l⁻**), which are somewhat less negative than the others.

Table 1. Potentials (vs. SCE) of active aldehydes (2^-)^[a] in deaerated MeCN determined by cyclic voltammetry, and adiabatic ionization potentials (I_p) and negative charge densities (ρ) on the oxygen and C2 carbon atoms calculated by the PM3 methods.



	R ¹	R ²	R	$E_{\text{ox}(1)}^0$ [V] ^[b]	$E_{\text{ox}(2)}^0$ [V] ^[b]	I_p [eV] ^[c]	ρ_{O}	ρ_{C2}
2a⁻	Me	H	<i>o</i> -MeC ₆ H ₄	-0.96	-0.52	1.78	-0.56	-0.65
2b⁻	Me	Me	<i>o</i> -MeC ₆ H ₄	-0.97	-0.56	1.68	-0.54	-0.69
2c⁻	H	H	<i>o</i> -MeC ₆ H ₄	-0.95	-0.50	1.70	-0.56	-0.64
2d⁻	Me	H	Naph	-0.96	-0.53	1.72	-0.54	-0.68
2e⁻	Me	H	An	-0.97	-0.42	1.87	-0.53	-0.68
2f⁻	Me	H	Ph	-0.78 ^[d]	-0.44 ^[d]	1.72	-0.54	-0.69
2g⁻	Me	Me	Ph	-0.79 ^[d]	-0.45 ^[d]	1.73	-0.54	-0.69
2h⁻	H	H	Ph	-0.77 ^[d]	-0.42 ^[d]	1.72	-0.55	-0.65
2i⁻	Me	H	Me	-0.98 ^[d]	-0.74 ^[d]	1.57	-0.56	-0.71
2j⁻	Me	Me	Me	-0.96 ^[d]	-0.73 ^[d]	1.56	-0.56	-0.71
2k⁻	H	H	Me	-0.93 ^[d]	-0.73 ^[d]	1.57	-0.56	-0.70
2l⁻	Me	H	<i>p</i> -CNC ₆ H ₄	-0.78 ^[d]	-0.44 ^[d]	1.96	-0.54	-0.68
2m⁻	Me	H	2,4-Cl ₂ C ₆ H ₃	-0.93 ^[d]	-0.41 ^[d]	1.83	-0.53	-0.68
2n⁻	Me	H	<i>p</i> -MeOC ₆ H ₄	-0.96 ^[d]	-0.64 ^[d]	1.72	-0.54	-0.69

[a] Active aldehydes **2a⁻**–**2n⁻** were prepared by adding neat DBU (1.0×10^{-2} M) to deaerated MeCN solution containing **1a⁻**–**1c⁺** (5.0×10^{-3} M), RCHO (0.25 M), and TBAP (0.10 M). Working electrode: Pt. Sweep rate: 0.10 V s^{-1} . [b] Measured at 298 K unless otherwise noted. [c] Calculated from the difference in the heat of formation (ΔH_f) between **2a⁻**–**2n⁻** and **2a⁻**–**2n⁻**. [d] Measured at 233 K.

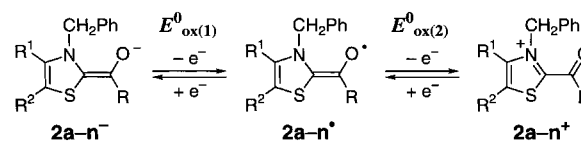
The adiabatic ionization potentials I_p and the negative charge densities ρ on the oxygen and C2 carbon atoms of **2a⁻**–**2n⁻** were calculated by using the semiempirical PM3 MO method (see Experimental Section);^[23] these too are listed in Table 1. Both the I_p and ρ values are also insensitive to the parent aldehydes, indicating that the HOMO levels and the solvation energies are about the same regardless of the parent. This may be the reason why the $E_{\text{ox}(1)}^0$ values are insensitive to the parent aldehydes, although the slight difference in the solvation may be reflected in the somewhat different $E_{\text{ox}(1)}^0$ values. The $E_{\text{ox}(1)}^0$ values in Table 1 support the proposal by Jordan et al. that the one-electron oxidation potential of the active aldehyde, which can reduce a flavin analogue, must be more negative than -0.67 V vs. SCE .^[7c]

The second oxidation potentials $E_{\text{ox}(2)}^0$ of **2a⁻**–**2n⁻** are more sensitive to the parent aldehydes than are the first oxidation potentials $E_{\text{ox}(1)}^0$ (Table 1). The more negative $E_{\text{ox}(2)}^0$ of **2i⁻**–**2k⁻**, derived from acetaldehyde, compared with those for other active aldehydes (Table 1) may be ascribed to the electron-releasing effect of methyl group that would stabilize the corresponding cations **2i⁺**–**2k⁺**.

Detection and characterization of radical intermediates: The observation of well-defined one-electron redox couples of active aldehydes (**2a⁻**–**2n⁻**) indicates that radical intermediates (**2a⁻**–**2n⁻**) are formed in the first one-electron oxidation of the active aldehydes. Therefore, the ESR spectrum of a radical intermediate (**2a[•]**, Scheme 2) generated by the controlled-potential electrolysis of **2a⁻** was measured in deaerated MeCN containing 0.10 M TBAP at 298 K (see Experimental Section). When the solution containing **2a⁻** was electrolysed at -0.70 V vs. SCE , which is between the first and second one-electron oxidation potentials, a radical species having a g

value of 2.0054 was detected successfully at 298 K as shown in Figure 2a. The signal disappeared when the solution was electrolysed at -1.20 and -0.30 V vs. SCE , values which correspond to the one-electron oxidation and reduction potentials, respectively, of **2a[•]**. The radical species **2d[•]** and **2e[•]**, derived from 1-naphthaldehyde and 9-anthraldehyde, were also observed at 298 K in the same manner (Figure 2e and 2f, respectively). The radicals derived from unstable active aldehydes at 298 K could also be detected after the controlled-potential electrolysis of the corresponding active aldehydes by keeping the reaction system at a low temperature (233 K) as in the case of CV measurements. The ESR spectra thus obtained are also shown in Figure 2.

The observed ESR spectra of active aldehyde radicals (**2a⁻**–**2n⁻**) can be simulated with the hyperfine splitting (hfs) values listed in Table 2, as shown in Figure 2. The hfs values indicate clearly that the active aldehydes exist in the anion form **2a⁻**–**2n⁻** where deprotonation of the hydroxy group occurs in the presence of a strong base such as DBU, since



Scheme 2. Oxidation of active aldehydes **2a⁻**–**2n⁻** by two electron-transfer steps.

no hyperfine splitting due to the hydroxy proton of the one-electron-oxidized radicals (**2a⁻**–**2n⁻**) is observed. Deuterium substitution at appropriate known sites may permit experimental verification of the assignment of the observed radical species, since a single deuterium gives a triplet (instead of doublet) hyperfine pattern and the deuterium splitting should decrease by the magnetogyric ratio of proton to deuterium (0.143).^[24, 25] In fact, deuterium substitution of the two hydrogen atoms at the benzylic position of **2a[•]** resulted in a drastic change in the splitting pattern from the spectrum in Figure 2a to that in Figure 2b, where **1a⁺** is replaced by 3-([α, α' -²H₂]benzyl)-4-methylthiazolium ion. The hfs value of 2.35 G resulting from PhCH₂ protons of **2a[•]** is decreased by the factor of the magnetogyric ratio of proton to deuterium (0.143) to 0.35 G due to the PhCD₂ deuterons of the corresponding deuterated radical (**2a[•]**(PhCD₂)). The change in the splitting pattern is also observed on deuterium substitution of two hydrogen atoms at the benzylic position of **2i[•]** (**2i[•]**(PhCD₂)) as well as that of the three hydrogen atoms of the acetyl moiety of **2i[•]** (**2i[•]**(CD₃CO)) shown in parts k–m of Figure 2. The hfs values of 2.34 and 3.46 G due to PhCH₂ and CH₃CO protons of **2d[•]** are decreased by factors of 0.143 to 0.33 and 0.51 G due to PhCD₂ and CD₃CO deuterons, respectively, while the other hfs values remain identical. The substitution of one hydrogen

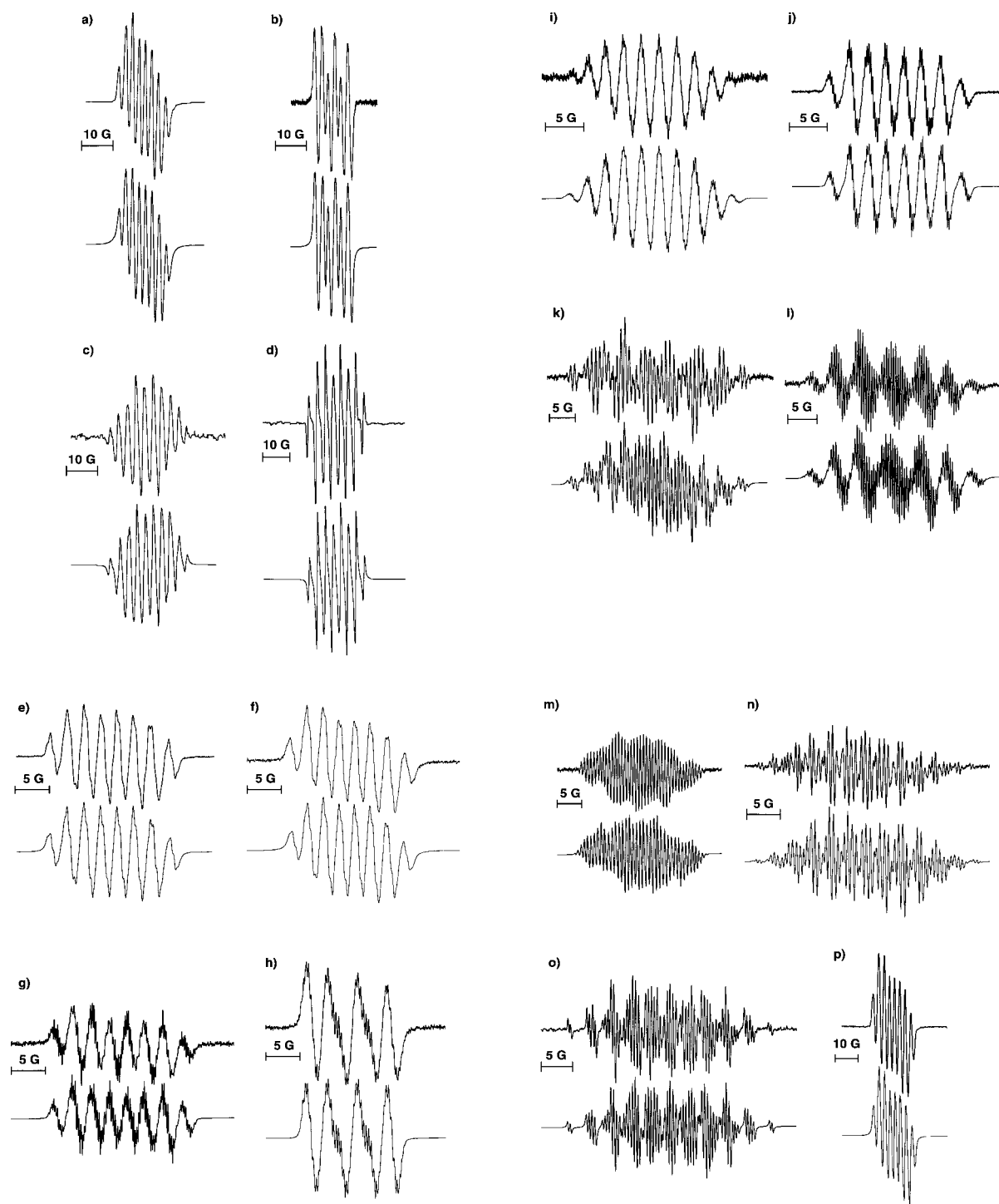


Figure 2. ESR spectra of active aldehyde radicals (2^{\bullet}) produced by the electrochemical oxidation of 2^- in deaerated MeCN containing 0.10 M TBAP and the computer simulation spectra: a) $2a^{\bullet}$, b) $2a^{\bullet}(\text{PhCD}_2)$, c) $2b^{\bullet}$, d) $2c^{\bullet}$, e) $2d^{\bullet}$, f) $2e^{\bullet}$, g) $2f^{\bullet}$, h) $2f^{\bullet}(\text{PhCD}_2)$, i) $2g^{\bullet}$, j) $2h^{\bullet}$, k) $2i^{\bullet}$, l) $2i^{\bullet}(\text{PhCD}_2)$, m) $2i^{\bullet}(\text{CD}_3\text{CO})$, n) $2j^{\bullet}$, o) $2k^{\bullet}$, and p) $2l^{\bullet}$. The hfs values used for the simulation are listed in Table 2.

atom with a methyl group at the C4 position of the thiazolium ring also causes a change in the splitting pattern (Figure 2). The above results confirm the assignment of the observed ESR signals to $2a^{\bullet}$ – l^{\bullet} in Table 2.

Thus, the one-electron oxidation of each active aldehyde leads to formation of the corresponding neutral radical, whose structure is similar to that suggested for the oxidized active aldehyde in pyruvate–ferredoxin oxidoreductase by Kerscher

and Oesterhelt.^[6b] The radical species $2a^{\bullet}$ – n^{\bullet} loses one more electron in the second oxidation to form the 2-acylthiazolium ions $2a^{\bullet+}$ – $n^{\bullet+}$ as depicted in Scheme 2.

An important point to note from the results in Table 2 is no or very small hfs values of the aromatic ring of active aldehyde radicals $2a^{\bullet}$ – h^{\bullet} and $2l^{\bullet}$ derived from aromatic aldehydes. This indicates no or little delocalization of spin on the aromatic ring. This is confirmed by the spin densities of $2a^{\bullet}$ and $2f^{\bullet}$,

Table 2. *g* Values and hyperfine splitting (hfs) values of active aldehyde radicals.

Radical	<i>g</i>	<i>a_N</i> (N)	<i>a_H</i> (PhCH ₂)	<i>a_H</i> (C4)	hfs [G]			
					<i>a_H</i> (C5)	<i>a_H</i> (CH ₃ CO)	<i>a_H</i> (C2')	<i>a_H</i> (C4')
2a[•]	2.0054	4.71 (4.73) ^[b]	2.35 (1.55) ^[b]	[a] (0.05) ^[b]	2.89 (2.59) ^[b]	– (<0.02) ^[b]	[a] (0.00007) ^[b]	[a]
2a[•](PhCD₂)	2.0054	4.71	0.35 ^[c]	[a]	2.89	–	[a]	[a]
2b[•]	2.0051	4.75	2.07	[a]	2.64	–	[a]	[a]
2c[•]	2.0053	4.89	2.66	[a]	2.66	–	[a]	[a]
2d[•]	2.0055	4.68	2.38	0.42	2.95	–	[a]	[a]
2e[•]	2.0055	4.74	2.35	0.50	2.89	–	–	[a]
2f[•]	2.0057	4.53 (4.89) ^[b]	2.40 (1.90) ^[b]	0.42 (0.03) ^[b]	3.10 (2.73) ^[b]	– (0.14) ^[b]	0.24 (0.12) ^[b]	0.48
2f[•](PhCD₂)	2.0057	4.53	0.35 ^[c]	0.42	3.10	–	0.24	0.48
2g[•]	2.0051	4.70	2.20	0.45	2.64	–	0.24	0.48
2h[•]	2.0057	4.66	2.48	0.42	2.83	–	0.21	0.43
2i[•]	2.0052	4.74	2.34	0.64	3.12	3.46	–	–
2i[•](PhCD₂)	2.0052	4.74	0.33 ^[c]	0.64	3.12	3.46	–	–
2i[•](CD₃CO)	2.0052	4.74	2.34	0.64	3.12	0.51 ^[c]	–	–
2j[•]	2.0052	5.02	2.24	0.50	2.85	3.54	–	–
2k[•]	2.0055	4.87	2.65	0.38	3.00	3.45	–	–
2l[•]	2.0055	4.48	2.30	0.50	2.93	–	[a]	[a]

[a] Too small to be determined. [b] The values in parentheses are those evaluated by the PM3 method. [c] Deuterium splitting value.

which were calculated by the PM3 method.^[23] The calculated hfs values based on the spin densities, which are given in parentheses in Table 2,^[26] agree reasonably well with the experimental values determined from the ESR spectra. The optimized structure of **2a[•]** with the SOMO orbitals is shown in Figure 3. The benzene ring of **2a[•]** derived from *o*-tolualdehyde is nearly perpendicular (87°) to the plane of the C=C double bond. This may be the reason why no spin is delocalized to the benzene ring in Figure 3. This is also consistent with the $E_{\text{ox}(1)}^{\circ}$ values being insensitive to the parent aldehydes.

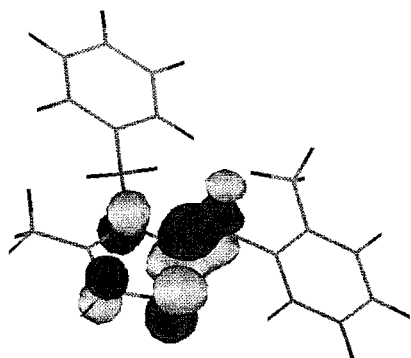
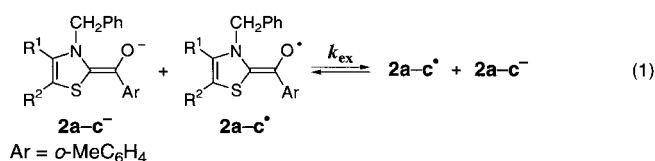


Figure 3. SOMO orbitals of **2a[•]** calculated by the PM3 method.

Reorganization energies of active aldehyde intermediates:

The linewidth variations of the ESR spectra of **2a–c[•]**, which are stable at 298 K, were used to investigate the electron-transfer exchange reactions between **2a–c[•]** and **2a–c[•]** [Eq. (1)].^[27] The active aldehydes **2a–c[•]** were prepared by



the addition of neat DBU to an MeCN solution of **1a–c⁺** and *o*-tolualdehyde, keeping the ratio of the components constant (**1a–c⁺**:*o*-tolualdehyde:DBU = 1:50:2). Then, the solution was partially electrolysed at –0.70 V vs. SCE, to give the corresponding radical species **2a–c[•]**. The maximum slope linewidths (ΔH_{msl}) were determined from the computer simulation of the ESR spectra (Figure 4). The ΔH_{msl} values of **2a–c[•]** thus determined increase linearly with an increase in the concentration of **2a–c[•]** as illustrated in Figure 5. The rate constants (k_{ex}) of the self-exchange reactions [Eq. (1)] were determined by means of Equation (2), where ΔH_{msl} and $\Delta H_{\text{msl}}^{\circ}$

$$k_{\text{ex}} = 1.52 \times 10^7 (\Delta H_{\text{msl}} - \Delta H_{\text{msl}}^{\circ}) / [(1 - P_i) [\text{2a-c}^\bullet]] \quad (2)$$

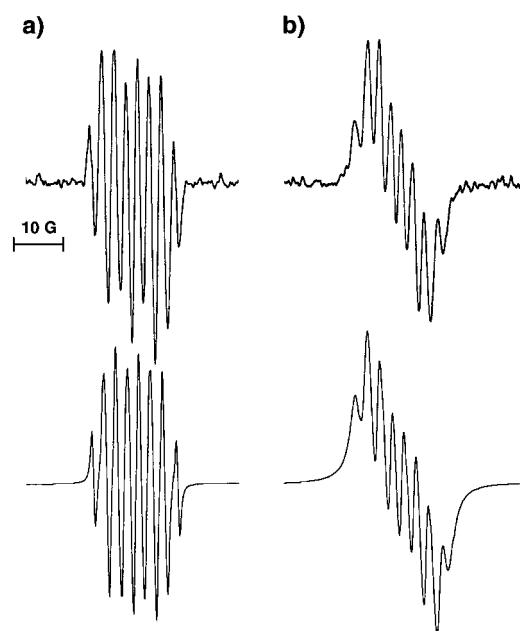


Figure 4. ESR spectra of $2a^\bullet$ in the presence of different concentrations of $2a^-$: a) 1.5×10^{-3} and b) 3.0×10^{-2} M in deaerated MeCN containing 0.10 M TBAP at 298 K, and the corresponding computer-simulated spectra from the hfs values shown in Table 4 and linewidths (ΔH_{msl}) of a) 0.50 and b) 1.55 G.

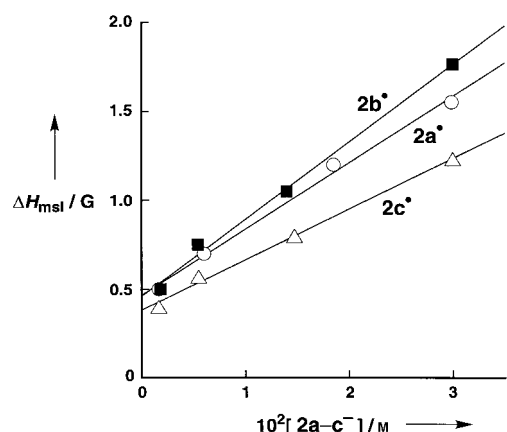


Figure 5. Plots of ΔH_{msl} of ESR spectra of $2a^\bullet$ (○), $2b^\bullet$ (■), $2c^\bullet$ (△) vs. $[2a^-c^-]$ in deaerated MeCN containing 0.10 M TBAP at 298 K.

are the maximum slope linewidths of the ESR spectra in the presence and absence of $2a^-c^-$, respectively, and P_i is a statistical factor which can be taken as nearly zero.^[28] The k_{ex} values thus determined are listed in Table 3.

The reorganization energies (λ) of the self-exchange reactions [Eq. (1)] were obtained from the k_{ex} values by means of Equation (3) ($Z = 10^{11} \text{M}^{-1} \text{s}^{-1}$);^[29] the λ values are

$$k_{\text{ex}} = Z \exp(-\lambda/4RT) \quad (3)$$

Table 3. Electron-exchange rate constants (k_{ex}) between $2a^-c^-$ and $2a^\bullet$, and experimental (λ) and calculated reorganization energies (λ_i) by the PM3 method.

Active aldehyde	$10^{-8}k_{\text{ex}}$ [$\text{M}^{-1}\text{s}^{-1}$]	λ [kcal mol ⁻¹]	λ_i [kcal mol ⁻¹]
$2a^-$	5.6	12.4	7.3
$2b^-$	6.6	12.0	11.4
$2c^-$	4.5	12.9	9.6

also listed in Table 3. No prominent change in the k_{ex} or λ values is observed dependent on the presence of methyl substituents on the thiazolium rings. The λ values are as small as those of fast electron-transfer exchange systems such as *p*-benzoquinone/semiquinone radical anion (13.1 kcal mol⁻¹ in DMF) and naphthalene/naphthalene radical anion (12.0 kcal mol⁻¹ in DMF).^[30]

The reorganization energies for the electron exchange between $2a^-$ and $2a^\bullet$ were theoretically evaluated with semiempirical PM3 MO calculations (see Experimental Section).^[23] The PM3-optimized structure of $2a^-$ was compared with that of the corresponding radical $2a^\bullet$, shown in Figure 6. Little structural change associated with the electron-transfer oxidation of $2a^-$ to $2a^\bullet$ is visible in Figure 6, although

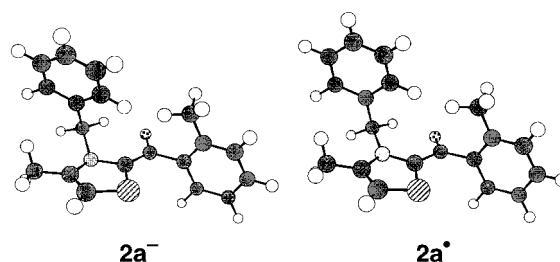


Figure 6. Optimized structures of $2a^-$ and the corresponding radical intermediate $2a^\bullet$ calculated by using the PM3 method.

the C=C double bond in $2a^\bullet$ (1.50 Å) becomes somewhat longer than that in $2a^-$ (1.39 Å). The difference between ΔH_f for $2a^\bullet$ with the unchanged structure from $2a^-$ and ΔH_f for $2a^\bullet$ with the optimized structure can be regarded as the reorganization energy of the inner coordination spheres (λ_i) associated with the structural change upon electron-transfer oxidation in the gas phase. Thus, the λ_i values of the $2a^-c^-/2a^\bullet$ system were calculated; the values are also listed in Table 3. The small λ_i values are consistent with little structural change accompanying the electron transfer. The difference between λ and λ_i indicates that solvent reorganization also plays a role in determining the intrinsic barrier to the electron transfer between $2a^-c^-$ and $2a^\bullet$.

Electron transfer from active aldehydes to an electron acceptor:

The small reorganization energies and the highly negative oxidation potentials of the active aldehydes indicate the high reducing ability to mediate electron transfer to an electron acceptor. This is confirmed by using tris(1,10-phenanthroline)cobalt(II) complex, $[\text{Co}^{\text{II}}(\text{phen})_3]^{2+}$ (phen = 1,10-phenanthroline), as an electron acceptor. This electron acceptor was chosen since the one-electron reduction potential ($E_{\text{red}}^\circ = -0.97$ V vs. SCE)^[31] is about the same as the one-electron oxidation potential of $2a^-$ ($E_{\text{ox}}^\circ = -0.96$ V vs. SCE) and the reorganization energy of the $[\text{Co}^{\text{II}}(\text{phen})_3]^{2+}/[\text{Co}^{\text{I}}(\text{phen})_3]^+$ system is small.^[31–33]

Upon addition of DBU (0.03 M) to a deaerated MeCN solution of $1a^+$ (2.0×10^{-4} M), *o*-tolualdehyde (0.03 M), and $[\text{Co}^{\text{II}}(\text{phen})_3]^{2+}$ (1.0×10^{-3} M) at 298 K, a new absorption band at 1415 nm due to the corresponding Co^{I} complex, $[\text{Co}^{\text{I}}(\text{phen})_3]^+$, appeared rapidly (Figure 7).^[34] In the absence of $1a^+$ and/or *o*-MeC₆H₄CHO, no formation of $[\text{Co}^{\text{I}}(\text{phen})_3]^+$ was observed. The formation of $[\text{Co}^{\text{I}}(\text{phen})_3]^+$ demonstrates

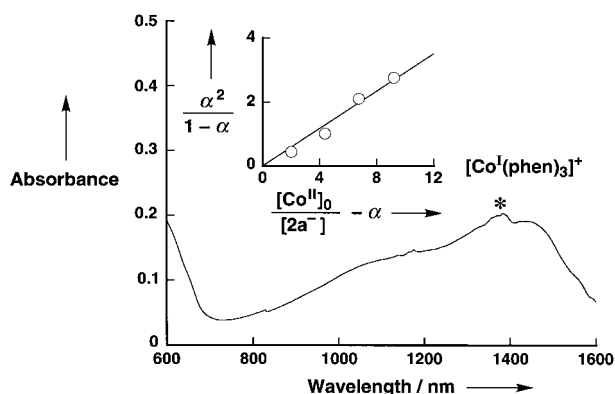
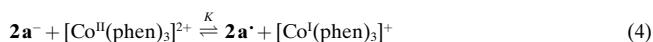


Figure 7. Visible–NIR spectrum observed after addition of DBU (0.03 M) to a deaerated MeCN solution of $\mathbf{1a}^+$ (2.0×10^{-4} M), *o*-tolualdehyde (0.03 M), and $[\text{Co}^{\text{II}}(\text{phen})_3](\text{PF}_6)_2$ (1.0×10^{-3} M) at 298 K. The peak marked with an asterisk is due to an artifact in the instrument. Inset: plot of $\alpha^2/(1-\alpha)$ vs. $([\text{Co}^{\text{II}}]_0/[\mathbf{2a}^-]_0 - \alpha)$; see text.

that the active aldehyde $\mathbf{2a}^-$, having a strong reducing ability, is formed in situ and acts as a good electron donor to reduce $[\text{Co}^{\text{II}}(\text{phen})_3]^{2+}$ [Eq. (4)].



The equilibrium constant (K) for the electron transfer between $\mathbf{2a}^-$ and the Co^{II} complex [Eq. (5)] is determined as 0.29 from the slope of the plot of $\alpha^2/(1-\alpha)$ vs. $([\text{Co}^{\text{II}}]_0/[\mathbf{2a}^-]_0 - \alpha)$ (in the inset of Figure 7) according to Equation (5), where α is the yield of the Co^{I} complex which is equal

$$\alpha^2/(1-\alpha) = K([\text{Co}^{\text{II}}]_0/[\mathbf{2a}^-]_0 - \alpha) \quad (5)$$

to $[\text{Co}^{\text{I}}]/[\mathbf{2a}^-]_0$, $[\text{Co}^{\text{I}}]$ is the concentration of $[\text{Co}^{\text{I}}(\text{phen})_3]^+$, and $[\mathbf{2a}^-]_0$ and $[\text{Co}^{\text{II}}]_0$ are the initial concentrations of $[\text{Co}^{\text{II}}(\text{phen})_3]^{2+}$ and $\mathbf{2a}^-$, respectively. From the K value, the one-electron oxidation potential of $\mathbf{2a}^-$ is determined as -0.94 V using Equations (6) and (7). This value agrees well with that obtained from the cyclic voltammogram (-0.96 V, in Table 1).

$$\Delta G_{\text{et}}^{\circ} = -RT \ln K \quad (6)$$

$$\Delta G_{\text{et}}^{\circ} = F(E_{\text{ox}}^{\circ} - E_{\text{red}}^{\circ}) \quad (7)$$

The rates of formation of $[\text{Co}^{\text{I}}(\text{phen})_3]^+$ in the electron transfer from $\mathbf{2a}^-$ to $[\text{Co}^{\text{II}}(\text{phen})_3]^{2+}$ were monitored by means of the increase of the absorbance due to $[\text{Co}^{\text{I}}(\text{phen})_3]^+$ at $\lambda = 426$ nm. The formation rates obeyed pseudo-first-order kinetics under conditions where the *o*- $\text{MeC}_6\text{H}_4\text{CHO}$ and DBU concentration was maintained at more than a tenfold excess of the $\mathbf{1a}^+$ and $[\text{Co}^{\text{II}}(\text{phen})_3]^{2+}$ concentrations. The observed pseudo-first-order rate constant (k_{obs}) for formation of $[\text{Co}^{\text{I}}(\text{phen})_3]^+$ is constant with the change in the *o*- $\text{MeC}_6\text{H}_4\text{CHO}$ concentration used in excess (Figure 8).

The rates of formation of $[\text{Co}^{\text{I}}(\text{phen})_3]^+$ were compared with those of formation of the active aldehyde intermediates determined from the increase in absorbance at $\lambda_{\text{max}} = 380$ nm due to $\mathbf{2a}^-$.^[7d–g] The rates obeyed pseudo-first-order kinetics under conditions where the *o*- $\text{MeC}_6\text{H}_4\text{CHO}$ and DBU con-

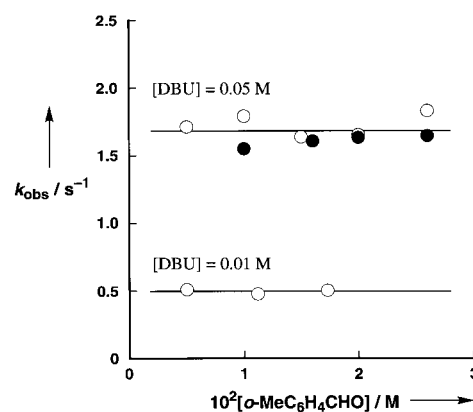
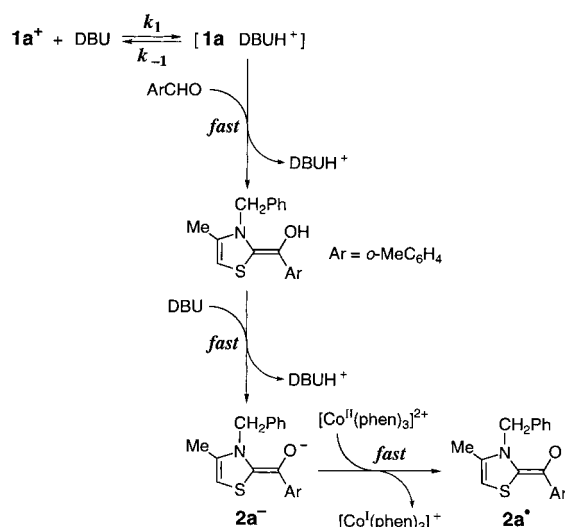


Figure 8. Plots of k_{obs} vs. $[o\text{-MeC}_6\text{H}_4\text{CHO}]$ for formation of $[\text{Co}^{\text{I}}(\text{phen})_3]^+$ in the electron-transfer reduction of $\mathbf{2a}^-$ with $[\text{Co}^{\text{II}}(\text{phen})_3]^{2+}$ (●) and for formation of $\mathbf{2a}^-$ (○) in deaerated MeCN at 298 K. $[\mathbf{1}^+] = 1.0 \times 10^{-3}$ M; $[\text{DBU}] = 0.01$ or 0.05 M.

centrations were maintained at more than a tenfold excess of the $\mathbf{1a}^+$ concentration. The observed pseudo-first-order rate constants for the formation of $[\text{Co}^{\text{I}}(\text{phen})_3]^+$ agree with those for formation of the active aldehyde ($\mathbf{2a}^-$) shown in Figure 8. Such an agreement demonstrates that the highly efficient electron transfer from $\mathbf{2a}^-$ to $[\text{Co}^{\text{II}}(\text{phen})_3]^{2+}$ occurs following the rate-determining formation of $\mathbf{2a}^-$, which is very strongly reducing. Since the k_{obs} values for formation of $\mathbf{2a}^-$ are constant with respect to changing *o*- $\text{MeC}_6\text{H}_4\text{CHO}$ concentration and increase with increasing DBU concentration (Figure 8), the rate-determining step for formation of $\mathbf{2a}^-$ and the electron transfer from $\mathbf{2a}^-$ to $[\text{Co}^{\text{II}}(\text{phen})_3]^{2+}$ may be the deprotonation of $\mathbf{1a}^+$ by DBU as sketched in Scheme 3. The rate constants (k_1) for deprotonation of $\mathbf{1a}^+$ were determined from the spectral change at 300 nm without aldehydes. The $k_1[\text{DBU}]$ values were then compared with the k_{obs} values for formation of active aldehyde ($\mathbf{2a}^-$) (Table 4). The k_{obs} values for formation of the active aldehyde $\mathbf{2a}^-$ at different DBU concentrations are essentially the same as the $k_1[\text{DBU}]$ values for deprotonation of $\mathbf{1a}^+$ by DBU in the absence of *o*-tolualdehyde. This agreement



Scheme 3. Mechanism of electron transfer from active aldehyde $\mathbf{2a}^-$ to $[\text{Co}^{\text{II}}(\text{phen})_3]^{2+}$.

Table 4. Observed pseudo-first-order rate constants (k_{obs}) for formation of active aldehydes ($2\mathbf{a}^-$), and forward rate constants $k_1[\text{DBU}]$ for deprotonation of ($1\mathbf{a}^-$) in deaerated MeCN at 298 K.

Thiazolium salt	[DBU] [M]	k_{obs} [s ⁻¹]	$k_1[\text{DBU}]$ [s ⁻¹]
$1\mathbf{a}^+$	0.01	0.41	0.41
	0.05	1.7	2.0
$1\mathbf{b}^+$	0.05	1.6	2.0
$1\mathbf{c}^+$	0.05	2.8	3.1

between the k_{obs} and $k_1[\text{DBU}]$ confirms that the active aldehydes are formed by rate-determining deprotonation of $1\mathbf{a}^-$ by DBU to afford the ylids $1\mathbf{a}^-$, followed by the subsequent rapid addition of $1\mathbf{a}^-$ to the aldehydes and the further deprotonation by DBU as depicted in Scheme 3 for the case of $1\mathbf{a}^+$.

As demonstrated above, thiazolium salts serve as efficient redox catalysts by forming the active aldehyde intermediates derived from various aldehydes in the presence of DBU. The largely negative one-electron oxidation potentials of the active aldehydes and the small reorganization energies for the electron-transfer reactions indicate that the active aldehydes have strong electron-donor abilities and that they are suitable for fast electron-transfer systems where they can act as efficient electron-transfer catalysts.

Experimental Section

Materials: Thiazolium salts ($1\mathbf{a}^+$: 3-benzyl-4-methylthiazolium bromide, $1\mathbf{b}^+$: 3-benzyl-4,5-dimethylthiazolium bromide, and $1\mathbf{c}^+$: 3-benzylthiazolium bromide) were prepared from the corresponding thiazole (4-methylthiazole, 4,5-dimethylthiazole, and thiazole, respectively) by reaction with benzyl bromide at 80 °C for 20 h, and purified by recrystallization from ethanol or acetone as described in the literature.^[18a] The deuterated compound 3-([α,α' -²H₂]benzyl)-4-methylthiazolium bromide was prepared by the reaction of thiazole and [α,α' -²H₂]benzyl bromide, which was obtained by reaction of [α,α' -²H₂]benzyl alcohol with HBr.^[35] [α,α' -²H₂]Benzyl alcohol was prepared by reduction of benzoic acid with LiAlD₄, obtained from Aldrich. Tris(1,10-phenanthroline)cobalt(II) hexafluorophosphate, [Co^{II}(phen)₃](PF₆)₂, was prepared by adding 3 equiv of 1,10-phenanthroline (monohydrate) to cobalt(II) chloride (hexahydrate) in ethanol followed by the addition of KPF₆ according to literature procedures.^[31, 36, 37] Aldehydes used in this study [*o*-tolualdehyde (*o*-MeC₆H₄CHO), 1-naphthaldehyde (NaphCHO), 9-anthraldehyde (AnCHO), benzaldehyde (PhCHO), acetaldehyde (MeCHO), *p*-cyanobenzaldehyde (*p*-CNC₆H₄CHO), 2,4-dichlorobenzaldehyde (2,4-Cl₂C₆H₃CHO), *p*-methoxybenzaldehyde (*p*-MeOC₆H₄CHO), [²H₄]acetaldehyde (CD₃CO)] and 1,8-diazabicyclo[5.4.0]undec-7-ene (DBU) were obtained from Tokyo Chemical Industry Co., Ltd. (Japan) and purified by the standard methods.^[38] Tetra-*n*-butylammonium perchlorate (TBAP) used as a supporting electrolyte was purchased from Sigma Chemical Co., purified by successive recrystallizations from ethanol, and dried under vacuum at 40 °C. Acetonitrile (MeCN) used as solvent was purchased from Wako Pure Chemical Ind. Ltd. (Japan), and purified by successive distillation over CaH₂ prior to use.

Spectral and kinetic measurements: Typically, DBU (2 μL , 1.3×10^{-5} mol) was added to a quartz cuvette (10 mm i.d.) which contained 3-benzyl-4-methylthiazolium bromide ($1\mathbf{a}^+$: 4.4×10^{-4} M) and *o*-tolualdehyde (1.2×10^{-2} M) in deaerated MeCN (3.0 mL) at 298 K. The corresponding active aldehyde ($2\mathbf{a}^-$) was formed. Similar experimental conditions were employed for formation of other active aldehydes. UV/Vis spectral change associated with formation of the active aldehyde was monitored with a Hewlett Packard 8453 diode array spectrophotometer. Kinetic measurements for formation of thiazolium ylides and active aldehydes were carried out with a Union RA-103 stopped-flow spectrophotometer under argon at

atmospheric pressure. The rates of formation of thiazolium ylides and active aldehydes were determined by monitoring the increase in the intensity of the absorption bands at 300 and 380 nm, due to the ylides and active aldehydes, respectively, under pseudo-first-order conditions where the concentrations of DBU and/or *o*-tolualdehyde were maintained at more than tenfold excess of the thiazolium salt concentration. Pseudo-first-order rate constants were determined by a least-squares curve fit carried out by means of a Macintosh personal computer. The first-order plots of $\ln(A_{\infty} - A)$ vs. time (A_{∞} and A are the final absorbance and the absorbance during the reaction, respectively) were linear for three or more half-lives with the correlation coefficient $\rho > 0.999$.

Reaction of the active aldehyde $2\mathbf{a}^-$ with [Co^{II}(phen)₃](PF₆)₂ was started by addition of DBU (13 μL , 8.7×10^{-5} mol) to a quartz cuvette (10 mm i.d.) which contained $1\mathbf{a}^+$ (2.0×10^{-4} M), *o*-tolualdehyde (0.03 M), and [Co^{II}(phen)₃](PF₆)₂ (1.0×10^{-3} M) in deaerated MeCN (3.0 mL) at 298 K. Visible–NIR spectral change associated with the reduction of [Co^{II}(phen)₃](PF₆)₂ was monitored with a Hewlett Packard 8453 diode array spectrophotometer or a Shimadzu UV-3100PC spectrophotometer. Kinetic measurements for formation of [Co^I(phen)₃]⁺ were carried out by means of a Union RA-103 stopped-flow spectrophotometer under argon at atmospheric pressure. The rates of formation of [Co^I(phen)₃]⁺ were determined by an increase in the absorption band intensity at 426 nm due to the Co^I complex.

Cyclic voltammetry: Typically, DBU (7.5 μL , 5.0×10^{-5} mol) was added to an electrochemical cell which contained $1\mathbf{a}^+$ (5.0×10^{-3} M), *o*-tolualdehyde (0.25 M), and TBAP (0.10 M) in deaerated MeCN (5.0 mL) under argon at atmospheric pressure. The first and second one-electron redox potentials of the active aldehyde ($2\mathbf{a}^-$) thus generated were determined at 298 K by the cyclic voltammograms measured under deaerated conditions with a three-electrode system and a BAS 100B electrochemical analyser. Similar experimental conditions were employed for the cyclic voltammetry (CV) measurements of $2\mathbf{b}^-$. An MeCN bath containing solid CO₂ was used to keep the reaction temperature at 233 K for the CV measurements of $2\mathbf{f}^-$. The working and counterelectrodes were platinum, while Ag/AgNO₃ (0.01 M) was used as the reference electrode. All potentials are reported in V vs. SCE. The $E_{1/2}$ value of ferrocene used as a standard is 0.37 V vs. SCE in MeCN under our solution conditions.^[39]

ESR measurements: Typically, DBU (7.5 μL , 5.0×10^{-5} mol) was added to an electrolysis cell which contained $1\mathbf{a}^+$ (5.0×10^{-3} M), *o*-tolualdehyde (0.25 M), and TBAP (0.10 M) in deaerated MeCN (5.0 mL) under argon at atmospheric pressure. The active aldehyde radical $2\mathbf{a}^{\cdot}$ was generated electrochemically at an applied potential of -0.7 V vs. SCE. The solution containing the radical was transferred to an ESR tube by means of a syringe which had earlier been purged with a stream of argon. The ESR spectra of $2\mathbf{a}^{\cdot}$ and other active aldehyde radicals generated electrochemically were measured at 298 K or 233 K with a JEOL X-band spectrometer (JES-RE1XE). It was confirmed that the ESR signals due to the active aldehyde radicals disappeared when the latter were reduced or oxidized at -1.2 or -0.3 V, respectively. The ESR spectra were recorded under nonsaturating microwave power conditions. The magnitude of modulation was chosen to optimize the resolution and the signal-to-noise (S/N) ratio of the observed spectra. The g values were calibrated with a Mn²⁺ marker, and the hyperfine splitting (hfs) values were determined by computer simulation on a Calleo ESR Version 1.2 program (Calleo Scientific Software Publishers) on a Macintosh personal computer.

Theoretical calculations: The theoretical studies used the PM3 molecular orbital method.^[23] The calculations were performed by using the MOLMOLIS program Ver. 2.8 (Daikin Industries, Ltd). Final geometries and energies were obtained by optimizing the total molecular energy with respect to all structural variables. The geometries of the radicals were optimized using the unrestricted Hartree–Fock (UHF) formalism. The heat of formation (ΔH_f) values of the radicals were calculated with the UHF-optimized structures by the half-electron (HE) method with the restricted Hartree–Fock (RHF) formalism.^[40] The adiabatic ionization potentials (I_p) were calculated as the difference in ΔH_f between the radical and the corresponding anion form. The reorganization energies of the inner coordination spheres (λ_i) associated with the structural change of active aldehydes upon the electron-transfer oxidation were calculated as the difference in ΔH_f of the radicals with the same structures as the anion forms and ΔH_f with the structures optimized by the UHF formalism.

Acknowledgments

This work was partially supported by a Grant-in-Aid for Scientific Research (No. 101008) from the Japan Society for the Promotion of Science and by a Grant-in-Aid for Scientific Research Priority Area (Nos. 10149230, 10131242, 10146232, and 10125220) from the Ministry of Education, Science, Culture and Sports, Japan.

- [1] a) R. Breslow, *J. Am. Chem. Soc.* **1958**, *80*, 3719; b) L. O. Krampitz, *Annu. Rev. Biochem.* **1969**, *38*, 213; c) R. Kluger in *The Enzymes*, Vol. 20 (Ed.: D. S. Sigman), 3rd ed., Academic Press, New York, **1992**, pp. 271–318; d) R. Kluger, *Chem. Rev.* **1987**, *87*, 863; e) A. Schellenberger, *Angew. Chem.* **1967**, *79*, 1050; *Angew. Chem. Int. Ed. Engl.* **1967**, *6*, 1024; f) *The Biochemistry and Physiology of Thiamin Diphosphate Enzymes* (Eds.: H. Bisswanger, A. Schellenberger), Intemann, Prien, Germany, **1996**; g) *The Biochemistry and Physiology of Thiamin Diphosphate Enzymes* (Eds.: H. Bisswanger, J. Ullrich), VCH, Weinheim, **1991**; h) *Thiamin Pyrophosphate Biochemistry* (Eds.: A. Schellenberger, R. L. Schowen), CRC, Boca Raton, FL, **1988**; i) *Thiamin: Twenty Years of Progress* (Eds.: H. Z. Sable, C. J. Gubler), New York Academy of Sciences, New York, **1982**.
- [2] a) F. Dyda, W. Furey, S. Swaminathan, M. Sax, B. Farrenkopf, F. Jordan, *Biochemistry* **1993**, *32*, 6165; b) X. Zeng, B. Farrenkopf, S. Hohmann, F. Dyda, W. Furey, F. Jordan, *Biochemistry* **1993**, *32*, 2704; c) I. Baburina, Y. Gao, Z. Hu, F. Jordan, S. Hohmann, W. Furey, *Biochemistry* **1994**, *33*, 5630; d) A. Brown, N. Nemeria, J. Yi, D. Zhang, W. B. Jordan, R. S. Machado, J. R. Guest, F. Jordan, *Biochemistry* **1997**, *36*, 8071; e) F. Guo, D. Zhang, A. Kahyaoglu, R. S. Farid, F. Jordan, *Biochemistry* **1998**, *37*, 13379.
- [3] a) S. Sun, G. S. Smith, M. H. O'Leary, R. L. Schowen, *J. Am. Chem. Soc.* **1997**, *119*, 1507; b) F. J. Alvarez, J. Ermer, G. Hübner, A. Schellenberger, R. L. Schowen, *J. Am. Chem. Soc.* **1995**, *117*, 1678; c) S. Sun, R. G. Duggleby, R. L. Schowen, *J. Am. Chem. Soc.* **1995**, *117*, 7317.
- [4] L. J. Reed, *Acc. Chem. Res.* **1974**, *7*, 40.
- [5] a) L. P. Hager, *J. Biol. Chem.* **1957**, *229*, 251; b) Y. A. Müller, G. E. Schulz, *Science* **1993**, *259*, 965.
- [6] a) K. Uyeda, J. C. Rabinowitz, *J. Biol. Chem.* **1971**, *246*, 3120; b) L. Kerscher, D. Oesterheld, *Eur. J. Biochem.* **1981**, *116*, 595.
- [7] a) F. Jordan, Z. H. Kudzin, C. B. Rios, *J. Am. Chem. Soc.* **1987**, *109*, 4415; b) F. G. Bordwell, A. V. Satish, F. Jordan, C. B. Rios, A. C. Chung, *J. Am. Chem. Soc.* **1990**, *112*, 792; c) X. Zeng, A. Chung, M. Haran, F. Jordan, *J. Am. Chem. Soc.* **1991**, *113*, 5842; d) G. Barletta, W. P. Huskey, F. Jordan, *J. Am. Chem. Soc.* **1992**, *114*, 7607; e) C. C. Chiu, K. Pan, F. Jordan, *J. Am. Chem. Soc.* **1995**, *117*, 7027; f) C. C. Chiu, A. Chung, G. Barletta, F. Jordan, *J. Am. Chem. Soc.* **1996**, *118*, 11026; g) G. L. Barletta, Y. Zou, W. P. Huskey, F. Jordan, *J. Am. Chem. Soc.* **1997**, *119*, 2356.
- [8] D. Hilvert, R. Breslow, *Bioorg. Chem.* **1984**, *12*, 206.
- [9] a) S. Shinkai, T. Yamashita, Y. Kusano, O. Manabe, *Tetrahedron Lett.* **1980**, *21*, 2543; b) S. Shinkai, T. Yamashita, Y. Kusano, O. Manabe, *J. Org. Chem.* **1980**, *45*, 4947; c) S. Shinkai, T. Yamashita, Y. Kusano, O. Manabe, *J. Am. Chem. Soc.* **1982**, *104*, 563.
- [10] a) S. Ohshima, N. Tamura, T. Nabeshime, Y. Yano, *J. Chem. Soc. Chem. Commun.* **1993**, 712; b) A. Takaki, K. Utsumi, T. Kajiki, T. Kuroi, T. Nabeshima, Y. Yano, *Chem. Lett.* **1997**, 75; c) K. Utsumi, Y. Nishihara, K. Hoshino, S.-I. Kondo, T. Nabeshima, Y. Yano, *Chem. Lett.* **1997**, 1081.
- [11] a) H. Inoue, K. Higashiura, *J. Chem. Soc. Chem. Commun.* **1980**, 549; b) H. Inoue, S. Tamura, *J. Chem. Soc. Chem. Commun.* **1985**, 141; c) H. Inoue, S. Tamura, *J. Chem. Soc. Chem. Commun.* **1986**, 858.
- [12] a) S.-W. Tam, L. Jimenez, F. Diederich, *J. Am. Chem. Soc.* **1992**, *114*, 1503; b) W.-W. Tam-Chang, L. Jimenez, F. Diederich, *Helv. Chim. Acta* **1993**, *76*, 2616; c) P. Mattei, F. Diederich, *Angew. Chem.* **1996**, *108*, 1434; *Angew. Chem. Int. Ed. Engl.* **1996**, *35*, 1341; d) P. Mattei, F. Diederich, *Helv. Chim. Acta* **1997**, *80*, 1555.
- [13] J. Grosby, R. Stone, G. E. Lienhard, *J. Am. Chem. Soc.* **1970**, *92*, 2891.
- [14] Y. Murakami, J.-I. Kikuchi, Y. Hisaeda, O. Hayashida, *Chem. Rev.* **1996**, *96*, 721.
- [15] L. M. Ferreira, H. T. Chaves, A. M. Lobo, S. Prabhakar, H. S. Rzepa, *J. Chem. Soc. Chem. Commun.* **1993**, 133.
- [16] M. Tazaki, M. Kumakura, S. Nagahama, M. Takagi, *J. Chem. Soc. Chem. Commun.* **1995**, 1763.
- [17] F. J. Leeper, D. H. C. Smith, *J. Chem. Soc. Perkin Trans. 1* **1995**, 861.
- [18] a) T. Ugai, R. Tanaka, T. Dokawa, *J. Pharm. Soc. Jpn.* **1943**, *63*, 296; b) W. Tagaki, H. Hara, *J. Chem. Soc. Chem. Commun.* **1973**, 891; c) J. A. Zoltewicz, J. K. O'Halloran, *J. Org. Chem.* **1978**, *43*, 1713; d) F. Diederich, H.-D. Lutter, *J. Am. Chem. Soc.* **1989**, *111*, 8438; e) Y.-T. Chen, G. L. Barletta, K. Haghjoo, J. T. Cheng, F. Jordan, *J. Org. Chem.* **1994**, *59*, 7714; f) K. Moteshareh, D. C. Myles, *J. Am. Chem. Soc.* **1997**, *119*, 6674.
- [19] a) R. Breslow, E. Kool, *Tetrahedron Lett.* **1988**, *29*, 1635; b) R. Breslow, R. Kim, *Tetrahedron Lett.* **1994**, *35*, 699; c) R. Breslow, C. Schmutz, *Tetrahedron Lett.* **1996**, *37*, 8241.
- [20] The oxidation peak potentials of *O*-methylated active aldehyde analogues have been reported to be in the range of –169 to +144 mV vs. SCE in DMSO. The formation of a radical cation intermediate upon the electrochemical oxidation is suggested based on chemical demonstration of formation of a dimer at the C2 α carbon; see: G. Barletta, A. C. Chung, C. B. Rios, F. Jordan, J. M. Schlegel, *J. Am. Chem. Soc.* **1990**, *112*, 8144.
- [21] Preliminary reports have appeared: a) I. Nakanishi, S. Itoh, T. Suenobu, S. Fukuzumi, *Angew. Chem.* **1998**, *110*, 1040; *Angew. Chem. Int. Ed.* **1998**, *37*, 992.
- [22] I. Nakanishi, S. Itoh, T. Suenobu, H. Inoue, S. Fukuzumi, *Chem. Lett.* **1997**, 707.
- [23] J. J. P. Stewart, *J. Comput. Chem.* **1989**, *10*, 209, 221.
- [24] J. E. Wertz, J. R. Bolton, *Electron Spin Resonance, Elementary Theory and Practical Applications*, McGraw-Hill, New York, **1972**.
- [25] S. Fukuzumi, Y. Tokuda, T. Kitano, T. Okamoto, J. Otera, *J. Am. Chem. Soc.* **1993**, *115*, 8960.
- [26] The hfs values of $a_{\text{H}}(\text{PhCH}_2)$ were evaluated from the 2s spin densities of **2a** \cdot and **2f** \cdot calculated by the PM3 method with the UHF formalism. The hfs values of $a_{\text{N}}(\text{N})$, $a_{\text{H}}(\text{C4})$, $a_{\text{H}}(\text{C5})$, $a_{\text{H}}(\text{C2}')$, and $a_{\text{H}}(\text{C4}')$ were estimated from the 2p $_z$ spin densities (ρ_i) calculated with the RHF formalism by using the relation $a_{\text{N}} = 25\rho_i$ and $a_{\text{H}} = 22.5\rho_i$.^[24]
- [27] I. Nakanishi, S. Itoh, T. Suenobu, S. Fukuzumi, *Chem. Commun.* **1997**, 1927.
- [28] a) R. L. Ward, S. I. Weissman, *J. Am. Chem. Soc.* **1957**, *79*, 2086; b) R. Chang, *J. Chem. Educ.* **1970**, *47*, 563; c) M. T. Watts, M. L. Lu, R. C. Chen, M. P. Eastman, *J. Phys. Chem.* **1973**, *77*, 2959; d) K. S. Cheng, N. Hirota, *Investigation of Rates and Mechanisms of Reactions*, Vol. VI (Ed.: G. G. Hammes), Wiley-Interscience, New York, **1974**, p. 565.
- [29] a) R. A. Marcus, *Annu. Rev. Phys. Chem.* **1964**, *15*, 155; b) R. A. Marcus, *Angew. Chem.* **1993**, *105*, 1161; *Angew. Chem. Int. Ed. Engl.* **1993**, *32*, 1111.
- [30] I. Ebersson, *Adv. Phys. Org. Chem.* **1982**, *18*, 79 and references therein.
- [31] C. V. Krishnan, B. S. Brunschwig, C. Creutz, N. Sutin, *Adv. Phys. Org. Chem.* **1985**, *107*, 2005.
- [32] R. Berkoff, K. Krist, H. D. Gafney, *Inorg. Chem.* **1980**, *19*, 1.
- [33] C. Creutz, H. A. Schwartz, N. Sutin, *J. Am. Chem. Soc.* **1984**, *106*, 3036.
- [34] $[\text{Co}^{\text{II}}(\text{phen})_3]^+$ was generated in the reduction of the Co^{II} complex by sodium amalgam in deaerated MeCN. Visible–NIR (MeCN), λ_{max} (nm) [$10^{-3}\epsilon$ ($\text{M}^{-1}\text{cm}^{-1}$)]: 426 [1.7], 1415 [4.7].
- [35] a) K. M. Doxsee, M. Feigel, K. D. Stewart, J. W. Canary, C. B. Knobler, D. J. Cram, *J. Am. Chem. Soc.* **1987**, *109*, 3098; b) V. Boekelheide, G. K. Vick, *J. Am. Chem. Soc.* **1956**, *78*, 653; c) W. G. Brown, *Org. React.* **1951**, 469; d) H. C. Brown, P. M. Weissmann, N. M. Yoon, *J. Am. Chem. Soc.* **1966**, *88*, 1458; e) G. J. Karabatsos, R. L. Shone, *J. Org. Chem.* **1968**, *33*, 619.
- [36] a) D. K. Liu, B. S. Brunschwig, C. Creutz, N. Sutin, *J. Am. Chem. Soc.* **1986**, *108*, 1749; b) D. J. Szalda, C. Creutz, D. Mahajan, N. Sutin, *Inorg. Chem.* **1983**, *22*, 2372.
- [37] F. H. Burstall, R. S. Nyholm, *J. Chem. Soc.* **1952**, 3570.
- [38] D. D. Perrin, W. L. F. Armarego, D. R. Perrin, *Purification of Laboratory Chemicals*, Pergamon, Elmsford, **1966**.
- [39] C. K. Mann, K. K. Barnes, *Electrochemical Reactions in Nonaqueous Systems*, Marcel Dekker, New York, **1990**.
- [40] T. Clark, *A Handbook of Computational Chemistry*, Wiley, New York, **1985**, p. 97.

Received: February 15, 1999 [F1618]